ELSEVIER

Nuclear Instruments and Methods in Physics Research B 182 (2001) 29–35

NIM B
Beam Interactions with Materials & Atoms

www.elsevier.com/locate/nimb

Binary contribution to the stopping in fast ion–surface collisions

M.S. Gravielle [a,b,*], D.G. Arbó [a,b], J.E. Miraglia [a,b]

[a] *Instituto de Astronomía y Física del Espacio (IAFE), Consejo Nacional de Investigaciones Científicas y Técnicas, C.C. 67, Suc. 28, 1428 Buenos Aires, Argentina*

[b] *Departamento de Física, FCEN, Universidad de Buenos Aires, Buenos Aires, Argentina*

Abstract

The mechanism of the binary collision with the free-electron gas in the proximity of a surface is investigated by employing a semiclassical formalism. The surface dynamic screening of the projectile is described with two well-known models commonly used in the literature: the parallel-dispersion (PD) and specular-reflection (SR) models. The Mermin–Lindhard dielectric function is used to represent the dielectric response of the bulk material. The formalism is applied to the calculation of the energy loss by fast protons colliding with an aluminum surface. Results are compared with those obtained with the dielectric formalism, and energy-loss distributions are analyzed. It is concluded that the models used to describe the dynamic screening potential do not seem to give a reliable description of the binary mechanism.

1. Introduction

When a fast ion grazingly collides with a metal surface, it loses energy as a consequence of the interaction with the conduction electrons of the solid. Two different mechanisms participate in this process: the excitation of the surface plasmon field and the binary electron excitation. While the first mechanism involves the collective response of the medium to the moving ion, the second one takes into account the single collisions of the projectile with the valence electrons, which compose the free-electron gas. In a previous work [1] we evaluated the binary collisions with the valence electrons by employing a semiclassical theory, in which the projectile trajectory is classically determined while the electronic transitions are tackled with quantum methods. In these calculations, a simple Yukawa-type potential was employed to represent the interaction between the projectile and the active electron, which is shielded by the presence of the other electrons of the free-electron gas.

The purpose of this work is to investigate the influence of the dynamic screening of the projectile on the binary mechanism in the proximity of a surface. With this goal in mind we introduce a more elaborated description of the effective projectile-electron potential in the collisional formalism, also called binary formalism (by *binary* we mean that the collisional system is composed of the projectile and one active electron bound to the surface). Two models are considered to represent the induced surface field:

* Corresponding author. Tel.: +54-11-47-81-67-55; fax: +54-11-47-86-81-14.

E-mail address: msilvia@iafe.uba.ar (M.S. Gravielle).

0168-583X/01/$ - see front matter
PII: S0168-583X(01)00651-6

the here-called parallel dispersion (PD) model, which is derived from the dielectric theory for semi-infinite media by neglecting the dispersion perpendicular to the surface [2,3], and the well-known specular-reflection (SR) model [4–6]. The binary results are compared with those calculated with the usual dielectric formulation [7,8], which takes into account single particle collisions *and* excitation of collective modes, without separating their contributions.

The collision system composed of 700 keV protons impinging on an aluminum surface is here used as benchmark for the theory. The considered energy corresponds to the high velocity range, i.e., $v_i > v_F$, where v_i is the projectile impact velocity and v_F is the Fermi velocity of the free-electron gas. At this energy, protons can be considered as bare ions along the whole trajectory [9–11]. In our calculations the free-electron gas is represented with the simple surface-jellium model, and the T-matrix element that describes the electronic transition is evaluated by using the first Born approximation. Atomic units are used unless otherwise stated.

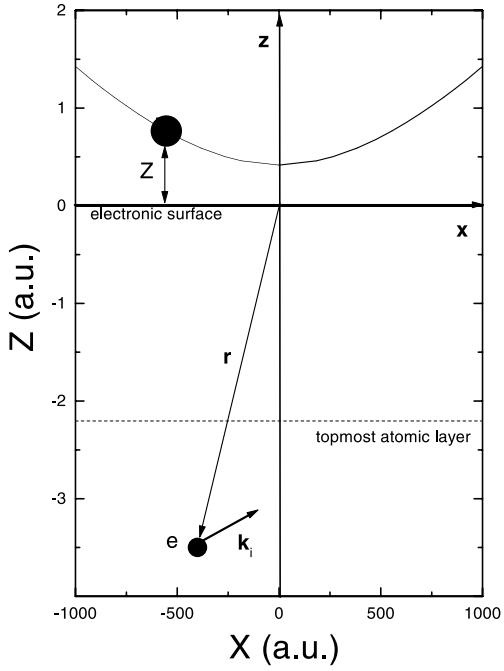

Fig. 1. Schematic picture of the co-ordinate system.

2. Theoretical models

We consider a heavy projectile (P) of charge Z_P grazingly impinging on a solid surface. As a result of the collision an electron (e) with initial momentum $\boldsymbol{k}_i$, belonging to the valence band of the solid, is excited to a state with momentum $\boldsymbol{k}_f$. We use a frame of reference fixed to the position of the electronic surface, which is placed at a distance $d/2$ in front of the first atomic layer, d being the interplanar separation. In this frame the classical projectile trajectory is contained in the x–z plane, and the surface in the x–y plane (see Fig. 1). Due to the symmetry of our problem, it is convenient to decompose the vectors into a two-dimensional vector parallel to the surface and a component perpendicular to the surface. In this way, the projectile velocity at the time t is written as $\boldsymbol{v} = (\boldsymbol{v}_s, v_z)$.

As we are interested in grazing collisions, the projectile trajectory can be divided into differential portions parallel to the surface at different distances Z. In every portion the component of the projectile velocity perpendicular to the surface v_z is considered negligible, and the ion moving parallel to the surface with velocity $\boldsymbol{v}_s$ collides with the individual electrons of the free-electron gas. Within this picture, the energy lost by the projectile per unit time reads [1]

$$S = 2\pi \int d\boldsymbol{k}_f \int d\boldsymbol{k}_i \rho_e \Theta(v_F - k_i)\Theta(k_f - v_F) \times E_{if}\delta(\Delta)|\mathscr{T}(\boldsymbol{k}_i, \boldsymbol{k}_f)|^2, \quad (1)$$

where $\mathscr{T}(\boldsymbol{k}_i, \boldsymbol{k}_f)$ is the T-matrix element corresponding to the inelastic transition $\boldsymbol{k}_i \to \boldsymbol{k}_f$. The delta function imposes the energy conservation, $\Delta = -E_{if} + \boldsymbol{v}_s \cdot (\boldsymbol{k}_f - \boldsymbol{k}_i)$, and $E_{if} = E_{\boldsymbol{k}_f} - E_{\boldsymbol{k}_i}$ is the energy gained by the electron (and lost by the projectile) in the collision. In Eq. (1) the unitary Heaviside function $\Theta(v_F - k_i)$ restricts the initial states to those contained inside the Fermi sphere, the function $\Theta(k_f - v_F)$ includes the Pauli exclusion principle, and $\rho_e = 2$ takes into account the spin states.

In the present work the T-matrix element is calculated with the first Born approximation. It reads $\mathscr{T}^{\mathrm{B}}(\boldsymbol{k}_{\mathrm{i}},\boldsymbol{k}_{\mathrm{f}}) = \langle \phi^{-}_{\boldsymbol{k}_{\mathrm{f}}} \mid V_{\mathrm{Pe}} \mid \phi^{+}_{\boldsymbol{k}_{\mathrm{i}}} \rangle$, where V_{Pe} is the Coulomb P–e interaction shielded by the presence of the other valence electrons, and $\phi^{+}_{\boldsymbol{k}_{\mathrm{i}}}(\phi^{-}_{\boldsymbol{k}_{\mathrm{f}}})$ is the initial (final) electronic state. Using the jellium model to represent the conduction band of the solid, the electronic wave functions can be written as $\phi^{\pm}_{\boldsymbol{k}}(\boldsymbol{r}) = (2\pi)^{-1}\exp(\mathrm{i}\boldsymbol{k}_{\mathrm{s}}\cdot\boldsymbol{r}_{\mathrm{s}})\varphi^{\pm}_{k_z}(r_z)$, where $\boldsymbol{r} = (\boldsymbol{r}_{\mathrm{s}}, r_z)$ is the position vector of the electron, $\boldsymbol{k} = (\boldsymbol{k}_{\mathrm{s}}, k_z)$ is the electron momentum inside the solid, and $E_{\boldsymbol{k}} = k_{\mathrm{s}}^2/2 + \epsilon_{k_z}$ is the electron energy. The sign $\pm$ indicates the incoming (−) and outgoing (+) asymptotic conditions, and the eigenfunctions $\varphi^{\pm}_{k_z}$ are defined in the Appendix of [1]. The T-matrix element $\mathscr{T}^{\mathrm{B}}(\boldsymbol{k}_{\mathrm{i}},\boldsymbol{k}_{\mathrm{f}})$ can be expressed as an integral in the momentum space

$$\mathscr{T}^{\mathrm{B}}(\boldsymbol{k}_{\mathrm{i}},\boldsymbol{k}_{\mathrm{f}}) = \frac{1}{(2\pi)^4}\int_{-\infty}^{+\infty} \mathrm{d}u\, \widetilde{V}_{\mathrm{Pe}}(u) f(u), \tag{2}$$

where $\widetilde{V}_{\mathrm{Pe}}(u)$ is the Fourier transform of V_{Pe} evaluated on $(\boldsymbol{p}_{\mathrm{s}}, u)$, $\boldsymbol{p} = \boldsymbol{k}_{\mathrm{f}} - \boldsymbol{k}_{\mathrm{i}} = (\boldsymbol{p}_{\mathrm{s}}, p_z)$ is the electron transferred momentum, and $f(u) = \langle \varphi^{-}_{k_{\mathrm{f}z}} \mid \exp(\mathrm{i}u r_z) \mid \varphi^{+}_{k_{\mathrm{i}z}} \rangle$ is the one-dimensional electronic form factor.

The function $\widetilde{V}_{\mathrm{Pe}}$ can be expressed as $\widetilde{V}_{\mathrm{Pe}}(u) = \widetilde{V}_{\mathrm{C}}(u) W_{\mathrm{Pe}}(u)$, where $\widetilde{V}_{\mathrm{C}}(u) = 2(2\pi)^2 Z_{\mathrm{P}}/(p_{\mathrm{s}}^2 + u^2)$ is the Fourier transform of the Coulomb P–e potential and $W_{\mathrm{Pe}}(u)$ is a screening factor, which plays the role of a sort of inverse dielectric function. We use two different approximations to describe the effective P–e potential: the PD and SR models. In the PD model, the screening factor $W_{\mathrm{Pe}}(u)$ reads [2,3]

$$\begin{aligned} W^{(\mathrm{PD})}_{\mathrm{Pe}}(u) &= \left[\frac{(1-\epsilon_{\mathrm{p}})}{(1+\epsilon_{\mathrm{p}})}\exp(-p_{\mathrm{s}}\,|\,Z\,|) + \exp(-\mathrm{i}uZ)\right]\Theta(Z) \\ &\quad -\frac{1}{\epsilon_{\mathrm{p}}}\left[\frac{(1-\epsilon_{\mathrm{p}})}{(1+\epsilon_{\mathrm{p}})}\exp(-p_{\mathrm{s}}\,|\,Z\,|) - \exp(-\mathrm{i}uZ)\right]\Theta(-Z), \end{aligned} \tag{3}$$

where ϵ_{p} is the bulk response function $\epsilon(\boldsymbol{q},\omega)$ evaluated on the momentum $\boldsymbol{q} = \boldsymbol{p}_{\mathrm{s}}$ and on the frequency $\omega = \boldsymbol{p}_{\mathrm{s}}\cdot\boldsymbol{v}_{\mathrm{s}}$, i.e. $\epsilon_{\mathrm{p}} = \epsilon(\boldsymbol{p}_{\mathrm{s}},\omega)$, with q_z drastically neglected. In the SR model, $W_{\mathrm{Pe}}(u)$ reads [4–6]

$$\begin{aligned} W^{(\mathrm{SR})}_{\mathrm{Pe}}(u) &= \left[\frac{\epsilon'_{\mathrm{s}}(u,0)\delta_{\mathrm{s}}^2 - p_{\mathrm{s}} - \mathrm{i}u\epsilon_{\mathrm{s}}(0)}{p_{\mathrm{s}}(1+\epsilon_{\mathrm{s}}(0))}\exp(-p_{\mathrm{s}}Z) + \exp(-\mathrm{i}uZ)\right]\Theta(Z) + \frac{\delta_{\mathrm{s}}^2}{p_{\mathrm{s}}}\left[\frac{\epsilon'_{\mathrm{s}}(u,Z)+\epsilon'_{\mathrm{s}}(u,-Z)}{2}\right. \\ &\quad \left. + \frac{\epsilon_s(Z)}{(1+\epsilon_{\mathrm{s}}(0))}\left(\frac{1}{p_{\mathrm{s}}+\mathrm{i}u} - \epsilon'_{\mathrm{s}}(u,0)\right)\right]\Theta(-Z), \end{aligned} \tag{4}$$

where $\delta_{\mathrm{s}}^2 = p_{\mathrm{s}}^2 + u^2$, and

$$\epsilon_{\mathrm{s}}(z) = \frac{p_{\mathrm{s}}}{\pi}\int_{-\infty}^{+\infty}\mathrm{d}q_z \frac{\exp(\mathrm{i}q_z z)}{(p_{\mathrm{s}}^2+q_z^2)}\frac{1}{\epsilon(\boldsymbol{p}_{\mathrm{s}}+q_z\widehat{z},\omega)}, \tag{5}$$

with $\epsilon(\boldsymbol{q},\omega)$ evaluated on the frequency $\omega = \boldsymbol{p}_{\mathrm{s}}\cdot\boldsymbol{v}_{\mathrm{s}}$. In Eq. (4) the function ϵ'_{s} is defined as $\epsilon'_{\mathrm{s}}(u,z) = \int_{-\infty}^{0}\mathrm{d}z'\exp(-\mathrm{i}uz')\epsilon_{\mathrm{s}}(z'-z)$. Note that $W^{(\mathrm{PD})}_{\mathrm{Pe}}$ can be derived from $W^{(\mathrm{SR})}_{\mathrm{Pe}}$ by neglecting the dependency on q_z of the bulk response function in Eq. (5), which leads to $\epsilon_{\mathrm{s}}(z) \simeq \epsilon_{\mathrm{p}}^{-1}\exp(-p_{\mathrm{s}}|Z|)$. In both models $\epsilon(\boldsymbol{q},\omega)$ is evaluated employing the random-phase approximation (Lindhard's dielectric function) together with Mermin's prescription, which allows us to deal with finite values of the lifetime $1/\gamma$.

3. Results

We confine our study to the collision system composed by 700 keV protons grazingly impinging on an Al(1 1 1) surface. The parameters used to describe the aluminum surface are: the Fermi energy $E_{\mathrm{F}} = 0.414$ a.u. ($v_{\mathrm{F}} = 0.91$ a.u.), the interplanar distance $d = 4.4$ a.u., the work function $E_{\mathrm{W}} = 0.15$ a.u., and the damping coefficient $\gamma = 0.037$ a.u. [12]. For the evaluation of S the five-dimensional integration on the momenta involved in Eq. (1) was resolved with the MonteCarlo numerical technique with a relative error less than 5%.

The energy loss per unit time S is plotted in Fig. 2 as a function of the projectile distance to the jellium edge. The PD and SR binary results are obtained from Eq. (1) employing the screened P–e potential given by the PD (Eq. (3)) and SR (Eq. (4))

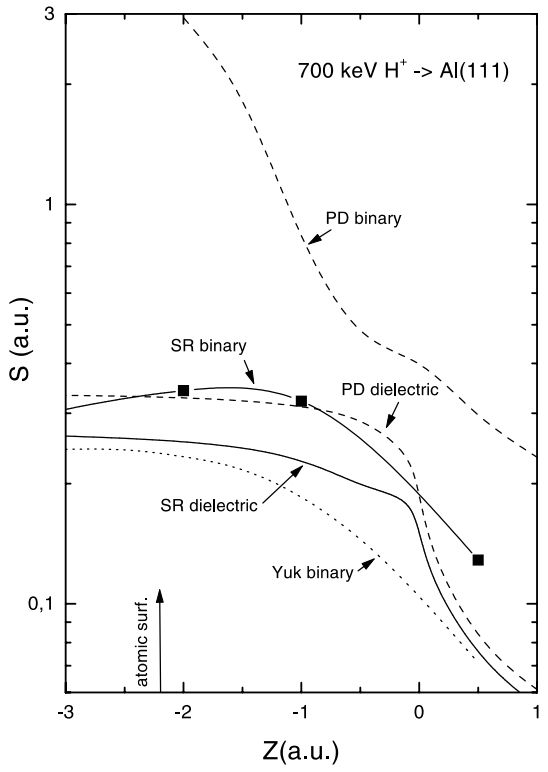

Fig. 2. Energy loss per unit time S as a function of the projectile distance Z to the electronic surface, for 700 keV protons impinging on an Al(1 1 1) surface. Solid lines, the binary collisional and dielectric contributions calculated with the SR induced potential, as explained in the text; and dashed lines, the binary collisional and dielectric contributions evaluated with the PD potential. The dotted line corresponds to the binary collisional results of [1] calculated with the Yukawa potential. The arrow indicates the position of the topmost atomic layer.

models, respectively. The SR binary results are displayed with full symbols, and the corresponding curve was obtained by interpolating the data together with the limit value inside the solid [13]. The calculation of the binary contribution to the energy loss within the SR model requires a huge computational effort, since the Fourier transform of the potential involves a further numerical integration given by Eq. (5). Just, only three results are presented, and the values have an error of around 10%. Besides the binary collisional data, in Fig. 2 we display the PD and SR dielectric results calculated within the full dielectric formalism using the corresponding induced potentials, i.e. [2, Eq. (3.19)] and [7, Eqs. (6)–(8)], respectively. Inside the solid our SR dielectric results coincide with the values of Juaristi et al. [7] obtained employing the same approximation (with slightly different parameters), but some differences are found in the vacuum region ($Z > 0$). Previous binary results from [1], which were calculated employing a Yukawa potential to represent the P–e interaction, are also shown in Fig. 2.

As the first point, it should be noted that the values obtained with the dielectric formalism do not seem to be very sensitive to the model used to describe the induced potential. The PD and SR dielectric curves have a similar shape, and the results almost coincide in the vacuum region, while inside the solid the differences are of the order of 30%. Lindhard's value (random-phase approximation) for the energy loss inside the solid ($S = 0.27$ a.u.) is quite well predicted by the SR dielectric model. The values obtained with the SR model within the *dielectric formalism* are expected to be quite reliable, and they can be considered as a reference.

However, serious problems are found for both PD and SR values obtained within the *binary formalism*, in the vacuum as well as in the subsurface region. For the vacuum ($Z > 0$), they largely run above their corresponding dielectric values. Since the dielectric formulation includes single-particle collisions plus plasmon excitations, the validity of these binary results is questionable. In other words, the binary contribution is expected not to exceed the total valence contribution given by the dielectric formalism.

Inside the solid ($Z < 0$), the PD binary values overestimate Lindhard's stopping by an order of magnitude, and therefore, they should be discarded. Instead, the SR binary results slowly tend to the half of the dielectric result deep inside the solid ($Z \to -\infty$), in agreement with the equipartition rule [14]. It states that the energy lost by the projectile is approximately ceded in equal parts to binary collisions and plasmon excitations. In solids, this rule is satisfied by the binary results when Lindhard's dielectric function is employed to describe the effective P–e potential [13]. Notice that the SR-induced potential (Eq. (4)) does tend to the wake potential given by the random-phase

approximation deep inside the solid ($Z \to -\infty$), while the PD potential (Eq. (3)) does not.

To study in detail the origin of the failure of the PD and SR models within the binary formalism, in Fig. 3 we plot the differential probability of energy loss dP/dE_{if} as a function of the lost energy E_{if}. The values of dP/dE_{if} are derived from Eq. (1) taking into consideration that S can be also expressed as $S = \int dE_{if} E_{if} (dP/dE_{if})$. Two different distances to the electronic surface are considered: $Z = -2$ and 0.5 a.u. Inside the solid, at $Z = -2$ a.u., the energy-loss distribution calculated with the PD model shows two peaks clearly situated at the surface and bulk plasmon frequencies shifted as a consequence of plasmon dispersion. Instead, the SR energy-loss distribution presents only one peak just at the surface plasmon frequency (Begrenzung effect) [5,6,15]. A similar enhancement was found by García de Abajo et al. [16,17] in the spectra of electron emission by binary collisions by using the same induced surface potential. The presence of the peak at the bulk plasmon frequency in the PD model is then the origin of the large discrepancy between PD and SR binary results inside the solid, as observed in Fig. 2. Outside the surface, at $Z = 0.5$ a.u., only a peak placed at the surface plasmon frequency is present in both PD and SR distributions. On the other side, no structure is present in the differential probability dP/dE_{if} obtained with the Yukawa potential. At high lost energies, all the models agree, indicating that they are describing head on (Coulomb) collisions.

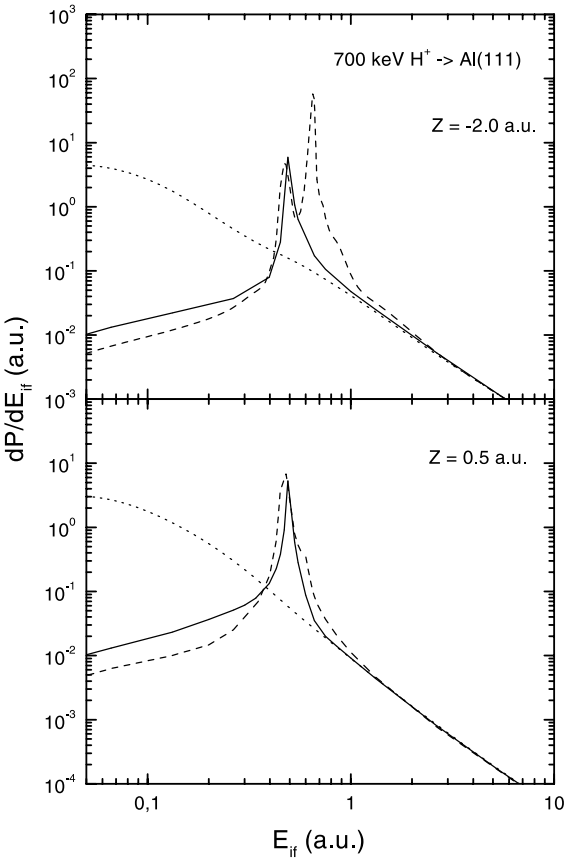

Fig. 3. Differential probability of energy loss by binary collisions dP/dE_{if} as a function of the lost energy E_{if}, for 700 keV protons impinging on an Al(1 1 1) surface. Two different projectile distances to the electronic surface are considered: $Z = -2$ and $Z = 0.5$ a.u. Solid and dashed lines represent the binary collisional contribution calculated with the SR and PD potentials, respectively. The dotted line corresponds to the energy loss obtained with the Yukawa potential.

At a first sight, one may be inclined to consider the peaks of the differential probability of energy loss by binary collisions as the transfer of energy to collective oscillations. However, this reading is *incorrect* because the binary formalism essentially describes the interaction between two particles, projectile and one active electron, therefore the collective absorption of energy is not contained in our formalism. The energy-loss distribution given by the SR model within the dielectric formalism (not shown here) indeed presents an enhancement at the surface plasmon frequency as a consequence of collective excitations, but we stress that this process is not included in the single kick mechanism described by our binary model.

Possible explanations for the presence of the peak observed in Fig. 2 are:

(i) such structure may be originated by the resonance of the electron scattered in the oscillatory pattern of the wake potential [5,6];
(ii) a deficiency of the first Born approximation used here; and
(iii) such structure may be an artifact of the calculation due to a simplification of the dielectric response function, as we explain next.

In the PD model, the failure could be adjudicated to the omission of the dispersion perpendicular

to the surface. Such an oversimplification implies that the z component of the transferred momentum p_z is considered null in the wake potential, while the description of the ion–electron collision given by Eq. (1) may take into account large values of p_z [18]. In the SR model, the description of the dispersion in the z direction is improved by considering the reflection of the perturbation at the surface. However, the SR potential is still expressed in terms of the bulk response function averaged on q_z (Eq. (5)), and the detailed information about the q_z distribution is lost.

The presence of an undesired enhancement in the binary energy-loss distribution is also found in the calculation of the stopping of ions within solids, where a full axial symmetry is present, when an inappropriate screening potential is employed [13]. In the bulk, the use of approximated dielectric functions such as plasmon pole approximation and related gives rise to a prominent peak in the binary energy-loss spectrum, which is nicely erased as Lindhard's dielectric function is used (see [13, Fig. 2]). Further, the energy loss obtained by adding all the binary collision probabilities coincides with the dielectric energy loss integrated on the binary region *only* if Lindhard's function is employed to describe the induced potential in the bulk. Note that in solids, plane waves are considered in both, electronic states and in the derivation of Lindhard's dielectric function. Instead, in collisions with surfaces a source of uncertainty arises from the fact that an *infinite* barrier is involved in the calculation of the SR model, while the jellium wave functions employed to describe the electronic states correspond to a *finite* barrier. This lack of self-consistency in the SR binary theory could also be the cause of the large difference between binary and dielectric results. It is then expected that a better description of the surface induced potential leads us to more precise results for the binary contribution.

In addition, it should be said that it is quite possible that the experimental electronic distributions indeed present an enhancement on the surface plasmon frequency. However, this enhancement cannot be a product of binary collisions as calculated here, but as a consequence of the decay of the surface plasmon after interacting with a single electron. This last process involves the collective response of the valence electrons, which is not considered in the binary formalism.

We conclude that the stopping of the projectile in grazing collisions with metal surfaces is not yet fully understood. The dielectric formalism seems to give an adequate description of the energy loss including the binary and collective processes, but problems arise when we try to separate the contribution of each mechanism. The binary collisional formalism, which is commonly used to calculate the induced electron emission [1,16, 17,19], strongly depends on the model employed to describe the surface wake potential. And not even the more elaborated SR model seems to give a reliable description of the P–e potential to deal with the binary mechanism. The deficiency of the binary results may come from an inconsistency between the wave functions employed to describe the electronic states and the surface-induced potential. Then, we expected that the calculation of the binary process can be improved by using surface electronic states in the derivation of screened potential within a quantum mechanical perturbation treatment.

References

[1] M.S. Gravielle, Phys. Rev. A 58 (1998) 4622.
[2] J. Burgdörfer, in: C.D. Lin (Ed.), Progress in Atomic and Molecular Physics, World Scientific, Singapore, 1993.
[3] C.O. Reinhold, J. Burgdörfer, Phys. Rev. A 55 (1997) 450.
[4] R.H. Ritchie, A.L. Marusak, Surf. Sci. 4 (1966) 234.
[5] F.J. García de Abajo, P.M. Echenique, Phys. Rev. B 46 (1992) 2663.
[6] F.J. García de Abajo, P.M. Echenique, Phys. Rev. B 48 (1993) 13399.
[7] J.I. Juaristi, F.J. García de Abajo, P.M. Echenique, Phys. Rev. B 53 (1996) 13839.
[8] Y. Wang, W.K. Liu, Phys. Rev. A 54 (1996) 636.
[9] H. Winter, R. Kirsch, J.C. Poizat, J. Remillieux, Phys. Rev. A 43 (1991) 1660.
[10] J.E. Miraglia, Phys. Rev. A 50 (1994) 2410.
[11] M.S. Gravielle, J.E. Miraglia, Phys. Rev. A 50 (1994) 2425, 3202.
[12] N.R. Arista, Phys. Rev. A 49 (1994) 1885.
[13] D.G. Arbó, J.E. Miraglia, Phys. Rev. A 58 (1998) 2970.
[14] J. Lindhard, A. Winther, Mat. Fys. Medd. Dan. Vid. Selsk. 34 (1964) 4.
[15] J.M. Cowley, Surf. Sci. 114 (1992) 587.

[16] F.J. García de Abajo, P.M. Echenique, Nucl. Instr. and Meth. B 79 (1993) 15.
[17] F.J. García de Abajo, Nucl. Instr. and Meth. B 98 (1995) 445.
[18] N. Stolterfoht, Nucl. Instr. and Meth. B 154 (1999) 13.
[19] M.L. Martiarena, E.A. Sánchez, O. Grizzi, V.H. Ponce, Phys. Rev. A 53 (1996) 895.